The International Journal of
Robotics Research

Clutchable series-elastic actuator: Implications for prosthetic knee design

Elliott J. Rouse, Luke M. Mooney and Hugh M. Herr

Clutchable series-elastic actuator: Implications for prosthetic knee design

Elliott J. Rouse[1], Luke M. Mooney[2] and Hugh M. Herr[1,3]

Abstract

Currently, the mobility of above-knee amputees is limited by the lack of available prostheses that can efficiently replicate biologically accurate movements. In this study, a powered knee prosthesis was designed utilizing a novel mechanism, known as a clutchable series-elastic actuator (CSEA).The CSEA includes a low-power clutch in parallel with an electric motor within a traditional series-elastic actuator. The stiffness of the series elasticity was tuned to match the elastically conservative region of the knee's torque-angle relationship during the stance phase of locomotion. During this region, the clutch was used to efficiently store energy in the series elasticity. The fully autonomous knee prosthesis design utilized a brushless electric motor, ballscrew transmission and cable drive, as well as commercial electrical components. The knee was lighter than the eighth percentile and shorter than the first percentile male shank segment. The CSEA Knee was tested in a unilateral above-knee amputee walking at 1.3 m/s. During walking, the CSEA Knee provided biomechanically accurate torque-angle behavior, agreeing within 17% of the net work and 27% of the stance flexion angle produced by the biological knee. In addition, the process of locomotion reduced the net electrical energy consumption of the CSEA Knee. The knee's motor generated 1.8 J/stride, and the net energy consumption was 3.6 J/stride, an order of magnitude less energy than previously published powered knee prostheses.

1. Introduction

1.1. Motivation

Transfemoral—or above-knee—amputees expend significantly more metabolic energy during walking than non-amputees (Waters and Mulroy, 1999). In addition, the majority of such amputees are dissatisfied with the extent they are able to use their prostheses (Christensen et al., 1995) and express lack of mobility as a chief concern (Legro et al., 1999). There is a need to develop highly efficient, lightweight powered leg prostheses that are able to provide biologically equivalent joint kinetics and kinematics. Such devices have the potential to restore natural movement patterns and substantially impact quality of life for such individuals.

The passivity of many knee prostheses is one cause of their shortcomings. Specifically, these prostheses typically incorporate hydraulic, pneumatic or friction elements and are limited in their ability to accommodate varying walking speeds and early-stance phase knee flexion. To address these limitations, quasi-passive knee prostheses use a microcontroller to vary the damping characteristics automatically throughout the gait cycle. Quasi-passive knees have been shown to increase self-selected walking speed as well as decrease peak vertical ground reaction force and metabolic cost, when compared to traditional passive knees (Segal et al., 2006; Kaufman et al., 2007; Johansson et al., 2005; Smith, 2007). Despite their benefits, neither passive nor quasi-passive knee prostheses can contribute positive mechanical energy. Hence they cannot replicate the positive power phases of the gait cycle, or assist in net-positive locomotion modes (i.e. stair or ramp ascent). Furthermore, extended use of these passive prostheses has been implicated in a number of gait asymmetries (Jaegers

[1]Media Arts and Sciences, Massachusetts Institute of Technology, USA
[2]Mechanical Engineering, Massachusetts Institute of Technology, USA
[3]Harvard-MIT Division of Health Science and Technology, USA

Corresponding author:
Elliott Jay Rouse, Massachusetts Institute of Technology, MIT Media Laboratory, 75 Amherst St, Cambridge, MA 02139, USA.
Email: erouse@media.mit.edu

et al., 1995; Johansson et al., 2005) and secondary disabilities (Lemaire and Fisher, 1994; Morgenroth et al., 2010, 2012), as well as failing to reduce the metabolic cost of locomotion to the level of non-amputees (Gitter et al., 1995; Waters and Mulroy, 1999).

Recent advancements in battery chemistry, brushless motor design and microprocessors have bolstered the development of autonomous and semi-autonomous powered prosthetic knees (Ossur (n.d.); Sup et al., 2008a, 2008b; Kapti and Yucenur, 2006; Martinez-Villalpando and Herr, 2009; Martinez-Villalpando et al., 2011). Sup et al. (2008a, 2008b) designed a powered knee and ankle prosthesis that used a finite-state impedance controller during locomotion, and more recently Ha et al. (2011) investigated volitional control of the same prosthesis using surface electromyography. This research is encouraging; however, the design of this prosthesis has no inherent elasticity, and is therefore subject to shock loads during use. Martinez-Villalpando and Herr (2009) and Martinez-Villalpando et al. (2008, 2011) presented an Active Agonist-Antagonist Knee Prosthesis, where dual series-elastic actuators (SEAs) actuated the knee joint in parallel to reduce the consumption of mechanical energy. A variable impedance control scheme was shown to qualitatively replicate able-bodied kinematics (Martinez-Villalpando and Herr, 2009); however, as a result of the dual, brushed actuators, improvements on the size, weight and efficiency of the prosthesis are possible. Lastly, Össur (n.d.) recently released the Power Knee; however, this prosthesis also has no inherent elasticity and has not been shown to provide substantial benefit to the intact limb (Wolf et al., 2013). Thus, despite promising previous work, the development of an energy-efficient, series-elastic knee prosthesis remains a challenge.

Early-stance knee flexion and extension—the phase of the knee angle profile following heel strike while bodyweight is borne by the leg—is an important portion of the gait cycle rarely seen in the gait of transfemoral amputees (Segal et al., 2006). Early-stance knee flexion is known to aid in shock absorption during heel contact (Gard and Childress, 2001), thereby reducing metabolic expenditure. The lack of this gait characteristic in transfemoral amputees may explain part of the increased metabolic cost of locomotion observed in this population. Thus, the development of future state-of-the-art robotic knee prostheses must be able to biomechanically replicate this important phase of locomotion.

1.2. Background

Over the past two decades, SEAs have been the focus of significant research in force-controlled robots (Pratt and Williamson, 1995; Pratt et al., 1997; Robinson et al., 1999; Pratt et al., 2002; Sensinger and Weir, 2005; Albu-Schaffer et al., 2008). A SEA includes a series compliance between the transmission output and the load, which has been shown to have substantial advantages. Such advantages include an increase in shock tolerance, limited high-frequency actuator impedance and energy storage, among other benefits (Pratt and Williamson, 1995; Pratt et al., 1997; Sensinger, 2006). Moreover, the series compliance increases force fidelity, a property especially useful in the impedance-controlled applications in fields such as wearable robotics and human-machine interfacing (Veneman et al., 2006; Au and Herr, 2008; Sensinger and Weir, 2008).

SEAs have been previously implemented in lower extremity prosthetic and exoskeleton devices. Au and Herr (2008) used series and parallel elasticity in the design of a powered ankle prosthesis, which was shown to lower the metabolic cost of walking in transtibial amputees (Au et al., 2009). In addition, Veneman et al. (2006) designed a lower extremity exoskeleton device using Bowden cable-driven SEAs. Recently, a new iteration of the design was proposed that used a direct-mounted SEA rather than the Bowden cable drive (Lagoda et al., 2010). As a result of the SEAs implemented in these designs, they have many favorable attributes; however, the cyclic and often spring-like torque-angle relationship observed during locomotion presents an opportunity to further innovate on the SEA architecture.

During the early-stance knee flexion and extension phase of human locomotion, the torque-angle relationship (Winter, 2009) is linear, or spring-like. A SEA implemented with a series stiffness approximately equal to the slope of this knee torque-angle relationship (often termed the quasi-stiffness (Rouse et al., 2013; Shamaei et al., 2013)) would provide a reduction in the mechanical work required by the motor within the SEA. In other words, the complete torque-angle relationship would be rendered by the physical spring alone, requiring only reactionary torque to be generated by the motor, at negligible motor speed. This provides a decrease in the mechanical energy required by the motor; however, because electric motors are inefficient at low speeds, an additional improvement may be made. In this investigation, we place a small clutch on the motor shaft to supply the reactionary torque on the motor's shaft when the actuator output dynamics are elastically conservative such as, for example, during the early-stance knee flexion-extension phase of human walking.

Previous researchers have investigated the use of clutchable elements in the design of wearable robotic actuators. Haeufle et al. (2012) introduced a clutched parallel-elastic actuator. In their work, a spring was incorporated in parallel to the electric motor and was engaged via a clutch. The purpose of the parallel spring was to augment the torque-angle characteristics of the mechanism passively. Such a design is advantageous because it enabled a reduced gear ratio and less powerful motor to be used, while maintaining the proper kinematics and kinetics of the stance phase. However, because there is no series compliance between the transmission output and the load, this mechanism cannot take advantage of the aforementioned beneficial properties of a SEA. Furthermore, because human locomotion includes spontaneous high-power modes (e.g. stair ascent and sit-to-stand transitions), it is essential for a prosthesis to be able to provide significant output power. Geeroms et

al. (2013) developed an ankle-knee prosthesis that uses two tuned stiffness elements at the knee with locking mechanisms to transfer energy from the knee to the ankle. This is an interesting design with substantial promise; however, as a result of the passive nature of the knee within this design, the device is limited to activities that do not require net positive work at the knee.

In this paper we introduce a new mechanism termed a clutchable series-elastic actuator (CSEA). The purpose of this device is twofold. Firstly, when the task dynamics are nonconservative, the CSEA offers all the benefits of a standard SEA, namely high-fidelity force control and enhanced motor-transmission protection from shock loads. Secondly, when the desired task dynamics are elastically conservative, the CSEA offers the ability to store elastic energy in the tuned series spring at low electrical power consumption. In the CSEA design, the small, low mass clutch placed on the motor shaft permits low electrical power consumption while providing the reactionary torque needed when the series spring is engaged during elastically conservative movement tasks. The architecture of this mechanism was motivated by the previous work of Herr et al. (2006) and Endo et al. (2006). In the work of Endo et al. (2006), agreement was shown between the kinetics and kinematics of an optimized quasi-passive, spring-clutch walking model and biomechanical data for humans ambulating across a level ground surface at 1.3 m/s. This work underscores the importance of tuned tendon compliance and isometric muscle contractions in human walking. We detail the mechanical design and control of a CSEA Knee prosthesis that is able to efficiently provide stance phase knee flexion during locomotion while expending minimal electrical energy. The CSEA Knee is tested with a transfemoral amputee during level ground walking at a self-selected speed.

2. Mechanism architecture and optimization

2.1. Electromechanical modeling

The CSEA mechanism is able to provide the benefits of a SEA while simultaneously providing a low-energy, elastic state when a mechanical clutch is engaged. Moreover, the series stiffness can be designed to provide a specific torque-angle relationship optimized for the dynamics of a particular task (i.e. the early-stance phase of walking). During this period of a conservative torque-angle relationship, the clutch is engaged to provide the reaction torque on the motor shaft, thereby bypassing the electric motor. The energetic economy stems from the difference in electrical energy required to provide the reaction torque (i.e. electric motors are known to be inefficient at low speeds). The CSEA mechanism consists of a series compliance (stiffness k_s) within a standard SEA with an added clutch in parallel with the motor (Figure 1). The engagement of the clutch alters the equations governing the mechanism. The motor's torque and displacement (τ and θ respectively, where subscripts m, l and c denote the motor, load and clutch,
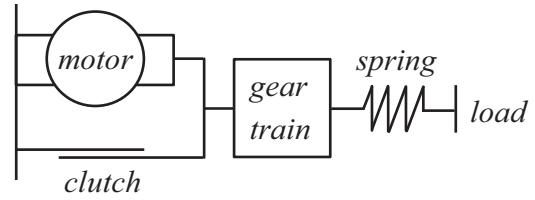
Fig. 1. Model of the clutchable series-elastic actuator. The clutch can be engaged, thereby bypassing the reaction torque required by the motor. This permits two mechanical states and the series compliance is tuned for the specific task.

respectively) can be written in terms of the task requirements (τ_l and θ_l), motor inertia (J_m), gear ratio (N) and efficiency (η) as follows:

$$\tau_m = \begin{cases} J_m \ddot{\theta}_m + \frac{\tau_l}{N\eta} & \text{clutch off} \\ 0 & \text{clutch on} \end{cases} \quad (1)$$

$$\theta_m = \begin{cases} \left(\frac{\tau_l}{k_s} + \theta_l\right)N & \text{clutch off} \\ \theta_c & \text{clutch on} \end{cases} \quad (2)$$

These equations provide a description of the motor's mechanical requirements for a specific task (i.e. specific τ_l and θ_l). To assess these requirements in terms of the electrical energy needed, the electrical motor model analogy was used to define motor current and voltage by

$$i_m = \begin{cases} \frac{\tau_m}{k_t} & \text{clutch off} \\ i_c & \text{clutch on} \end{cases} \quad (3)$$

$$v_m \begin{cases} \frac{R_m J_m}{k_t}\ddot{\theta}_m + \frac{\dot{\theta}_m}{k_v} + \frac{R_m}{k_t}\tau_m & \text{clutch off} \\ v_c & \text{clutch on} \end{cases} \quad (4)$$

where k_t is the torque constant of the motor, R_m is the winding resistance and k_v is the speed constant of the motor. Finally, the electrical power, p_m, is defined by

$$p_m = i_m v_m \quad (5)$$

Regeneration of negative electrical power was assumed through the use of modern four quadrant motor drives. By substituting (1) and (2) into (3)–(5), the mechanical and electrical characteristics of the CSEA mechanism can be quantified as a function of the task. These equations were used to model the performance of the CSEA mechanism in simulation.

2.2. Simulation

The CSEA mechanism was modeled for use in a robotic knee prosthesis and the series stiffness and potential energetic economy were quantified. A knee prosthesis was chosen because there is a portion of the stance phase of walking that is able to take advantage of the CSEA architecture. That is, during early-stance phase knee flexion and extension, the knee torque-angle relationship is predominantly spring-like in behavior (Figure 2). In addition, this
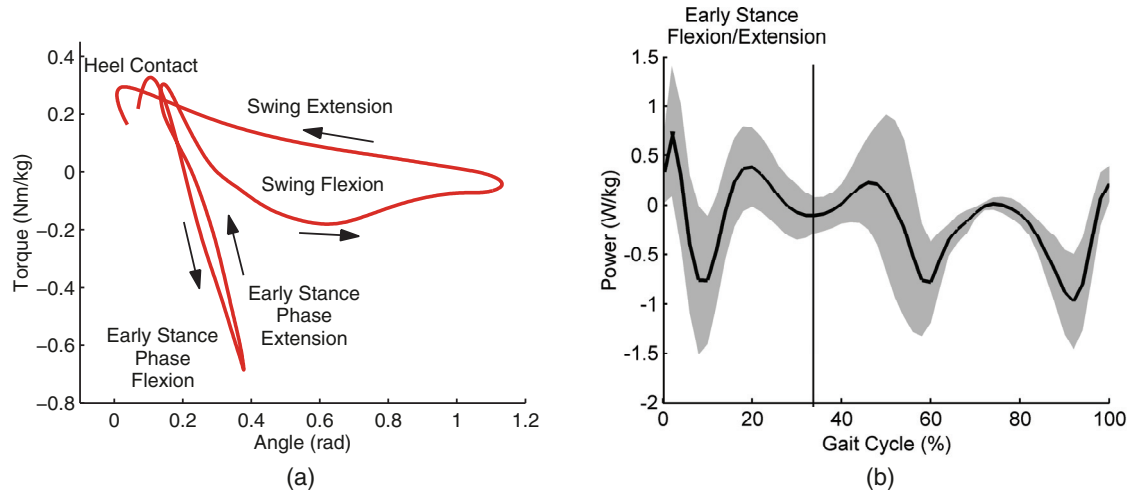
Fig. 2. (a) Knee torque-angle relationship during walking at self-selected speed, shown with salient features of the gait cycle denoted. Early-stance phase flexion and extension is predominantly linear and the dynamics can be replicated by a tuned spring. Data from Winter (1983). (b) Mechanical power of the knee shown throughout the gait cycle. The early-stance flexion and extension period terminates at approximately 35% of the gait cycle and includes the greatest regions of peak power. Bold denotes intersubject average with standard deviation shown in translucent.

Table 1. Clutchable series-elastic actuator model parameters.

Parameter	Symbol	Value
Motor inertia	J_m	33.3 gcm^2
Gear ratio	N	143
Mechanical efficiency	η	0.9
Torque constant	k_t	20.6 mNm/A
Speed constant	k_v	48.8 rad/s/V
Winding resistance	R_m	0.21 Ω
Clutch current	i_c	0.25 A
Clutch voltage	v_c	24 V
Series stiffness	k_s	240 Nm/rad

region consists of substantial positive (and negative) mechanical power phases during the gait cycle, further demonstrating the potential of the CSEA mechanism (Figure 2).

Representative, weight-normalized human locomotion data were used for 65, 75 and 85 kg persons walking at slow, self-selected and fast speeds across level ground (stride durations were 1.3, 1.1 and 1.0 s, respectively) (Winter, 1983). The knee torque and angle information were used as the load specifications, and Equations (1)–(5) were used to quantify motor kinetic and kinematic performance. Mechanism parameters used are listed in Table 1 (see Section 3 for rationale). The data were kinetically clamped—where the output torque, τ_l is fixed—and the clutch was activated during early-stance phase knee flexion/extension (activated/deactivated at the nearest point of zero velocity). The result of the simulation was the electrical energy profiles required to achieve the desired kinetics and kinematics, as well as the output knee angle that resulted from the use of the clutch. The

simulation was repeated for varying values of series stiffness. It should be noted that in this analysis, each configuration of stiffness yielded essentially identical electrical power profiles, but very different knee kinematics. The electrical power profiles were nearly identical because the clutch required a constant electrical power during operation when the stiffness greatly affected the knee angle displacement. Hence, the focus of the comparison was kinematic similarity rather than electrical energy. The scalar kinematic agreement was defined by

$$\psi = \int (\theta_{CSEA} - \theta_l)^2 dt \qquad (6)$$

where θ_{CSEA} is the output displacement of the CSEA and the load displacement, θ_l, is the reference knee angle; lastly, the function was integrated over the duration of each gait cycle. The agreement was quantified across subjects' weights and walking speeds (Figure 3(a)). The softer series stiffness caused substantial knee flexion values beyond the profiles acquired during level ground walking, whereas the greater stiffness values tracked the kinematics more closely (by essentially eliminating stance knee flexion), but reduced the benefits of including the series elasticity. Based on this analysis and available compression springs (see Section 3), the stiffness implemented in the CSEA knee was chosen to be 240 Nm/rad. The kinematic agreement, ψ, at this stiffness was 0.3 ± 0.3 rad^2 s.

To investigate the effect of the clutch in the CSEA, simulation experiments were performed for prosthetic knee mechanisms that both included the clutch (CSEA) and did not include the clutch (standard SEA). The computational model of the CSEA knee was tested across walking speeds and averaged across subject weights
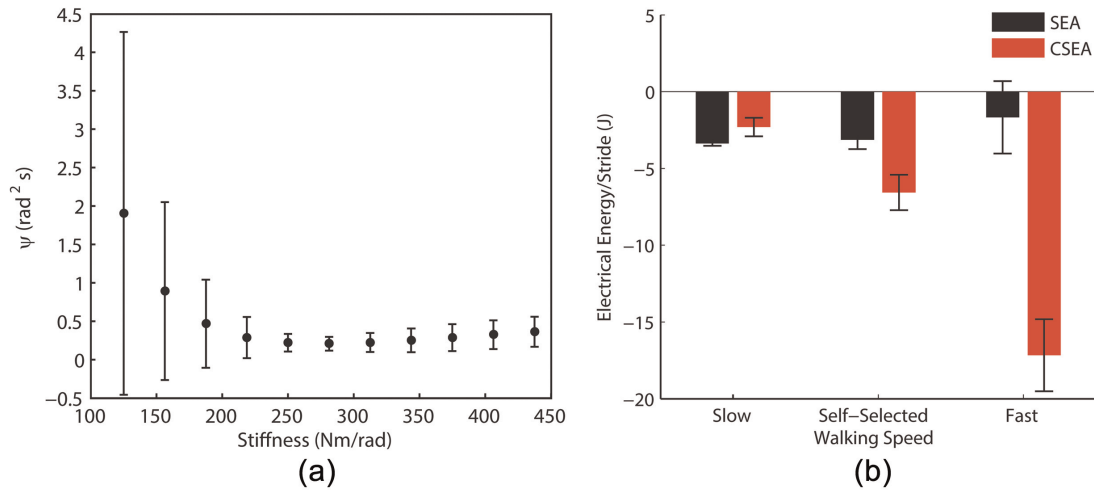
Fig. 3. (a) Kinematic error of simulation as a function of series stiffness, averaged across walking speeds and subject weights. Note the minimum at approximately 250 Nm/rad. (b) Electrical energy required for series-elastic mechanisms that include the clutch (red) and do not include a clutch (black), averaged across subject weights. The energy generated by the clutchable series-elastic actuator (CSEA) increases with speed while it decreases with a traditional SEA. Negative energy denotes generation and error bars are standard deviation.

(Figure 3(b)). On average, the CSEA generated 3.3 ± 5.2 times more energy when compared to a traditional SEA during walking. During slow walking speeds, the SEA generated more energy because the 6 W clutch within the CSEA required more energy than the motor of the traditional SEA. However, as speed increased, the clutch became substantially more efficient as the motor power demands of early-stance phase knee flexion increased. Therefore, the potential energetic savings of the CSEA mechanism is substantial in the context of a prosthetic knee.

3. Clutchable series-elastic actuator knee design

The CSEA Knee was designed to provide biomechanically relevant kinetics and kinematics in an anthropomorphic envelope. A target benchmark was chosen based on a 100 kg person under fast walking conditions, while fitting in the biological form factor of a 10th percentile male. These biomechanical requirements were determined from the weight-normalized representative kinematics and kinetics (Winter, 1991). It was assumed that the knee prosthesis would account for 75% of the length and mass between the knee and ankle joints, which was approximated as 3.5% of total body mass (Winter, 1991). The resulting specifications are shown in Table 2. These requirements provided the foundation for the mechanical design of the CSEA Knee.

The CSEA Knee was actuated by a custom (40 mm front shaft extension) 200 W brushless direct current (DC) motor (model: 305015, Maxon Motor, Sachseln, CH) and a 6 W electromagnetic clutch (model: 02.02.130, KEB, Barntrup, DE). The stall torque of the 36 V brushless motor was 3.5 Nm, and the maximum

Table 2. Clutchable series-elastic actuator mechanical design specifications.

Parameter	Value
Range of motion	0–1.2 radians
Static max torque	120 Nm
Dynamic max torque	40 Nm
Max positive power	100 W
Max negative power	210 W
Mass	<3000 g
Length	<323 mm

holding torque for the 24 V electromagnetic clutch was 0.75 Nm. The clutch was placed on the shaft of the brushless motor and together they actuated the ballscrew. The parallel motor and clutch drove the ballscrew via a GT2 timing belt with a 2 mm pitch and 6 mm width. The motor pulley had 22 teeth (model: A 6D51M022DF0605, Stock Drive Products/Sterling Instrument, New Hyde Park, NY), and the ballscrew pulley has 60 teeth (model: GPA60GT2060-B-P8-NFC, Misumi USA, Addison, IL).

The CSEA Knee was designed to have an angular series stiffness of 240 Nm/rad for 0.35 rad of flexion, as motivated by the simulations in Section 2.2. Two compression die springs under no preload were used as the elastic elements in the CSEA Knee. Compression springs were chosen over extension and torsional springs, since they typically exhibit higher volumetric and mass energy densities. Figure 4 shows how linear compression springs were implemented to create a rotational stiffness around the knee joint. The extension and flexion springs were sized to meet the required stiffness and energy storage while minimizing volume and mass. The rotational stiffness of the knee joint
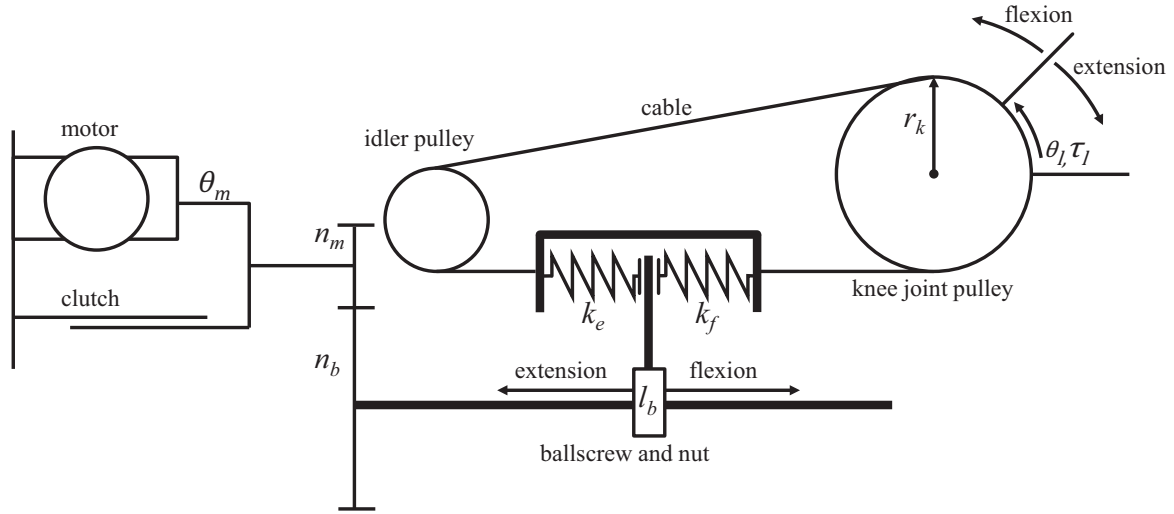
Fig. 4. The geometric configuration of the clutchable series-elastic actuator knee is depicted. The parallel motor and clutch were connected to a drive pulley with n_m teeth that drive the ballscrew pulley with n_b teeth. A ballscrew, with lead l_b, drives a ball nut between the extension and flexion compression springs with respective stiffnesses of k_e and k_f. The series-elastic housing drives the knee joint pulley, with radius r_k, via a drive cable.

and the linear stiffness of the compression springs are related by

$$k_s = \begin{cases} k_f r_k^2 & \tau_k > 0 \\ k_e r_k^2 & \tau_k < 0 \end{cases} \qquad (7)$$

Equation (7) shows that the radius of the knee joint, and consequently the length of ball nut travel and overall size of the prosthesis, was reduced as the stiffness of the compression spring increases. Therefore, the stiffest commercially available compression springs were chosen. The knee extension spring, which exerted the extension moment during early-stance flexion, had a stiffness of 385 N/mm (model: CV1250-1500-200, Associated Spring Raymond, Maumee, OH). A shorter spring with a similar stiffness of 338 N/mm was chosen for the flexion side (model: CV1000-1000-158, Associated Spring Raymond). A shorter spring was chosen for the flexion side because it was not typically required to store as much elastic energy. The spring constants differ by 12% due to the manufacturer stiffness availability given the geometric constraints.

The design of the knee joint pulley and linear actuator were both directly influenced by the stiffness of the series compression spring. The desired angular stiffness of 240 Nm/rad, the extension spring stiffness of 385 N/mm and (7) resulted in the 25 mm radius of the knee joint pulley (r_k). The radius of the knee joint pulley was subsequently used to determine the appropriate travel of the spring housing and ball nut. A 10 mm diameter ballscrew and nut assembly (model: ECN-10030-RZN, Nook Industries, Cleveland, OH), with a lead (l_b) of 3 mm, was used to efficiently and compactly transform the rotational motion of the motor to the linear compression of the series springs. The ballscrew and nut had a maximum dynamic

load rating of 2800 N and a maximum static load rating of 5000 N. Therefore, including the 25 mm radius of the knee joint, the ballscrew was able to exert a dynamic moment of 70 Nm, and a static moment of 125 Nm. Ballscrew and nut assemblies also have the added advantage of being backdrivable, which allowed the motor to act as a generator during periods of negative mechanical work. The overall transmission ratio (N) from the motor and clutch to the knee joint was

$$N = \frac{\dot{\theta}_m}{\dot{\theta}_l} = \frac{\tau_l}{\tau_m} = \left(\frac{n_b}{n_m}\right)\frac{2\pi r_k}{l_b} \qquad (8)$$

where n_b and n_m are the number of teeth on the ball screw pulley and motor/clutch pulley. Equation (7) resulted in a total transmission ratio of $N = 143$.

The architecture of the CSEA Knee was designed to handle the loads and moments of level ground walking, while minimizing weight and length in a biological form factor. A geometrically accurate schematic of the CSEA Knee's major components is shown in Figure 5. An important design constraint was the relative positioning of the ballscrew, series-elastic carriage and drive cables. The ballscrew was placed symmetrically between the two drive cables and the axes of the springs are colinear with the axis of the ballscrew. Two linear rails, each with two ballbearing blocks (model: SE2B-N6-100-WC, Misumi USA), aligned the series-elastic housing with the axis of the ballscrew. Two additional linear rails and sets of bearing blocks constrained the ball nut to axial translation within in the series-elastic housing. This arrangement reduced off-axis forces on the ball nut and limited the loads on the linear bearings to include only reactionary moments of the ball nut. The knee joint was mechanically limited to 0–2.1 radians by an
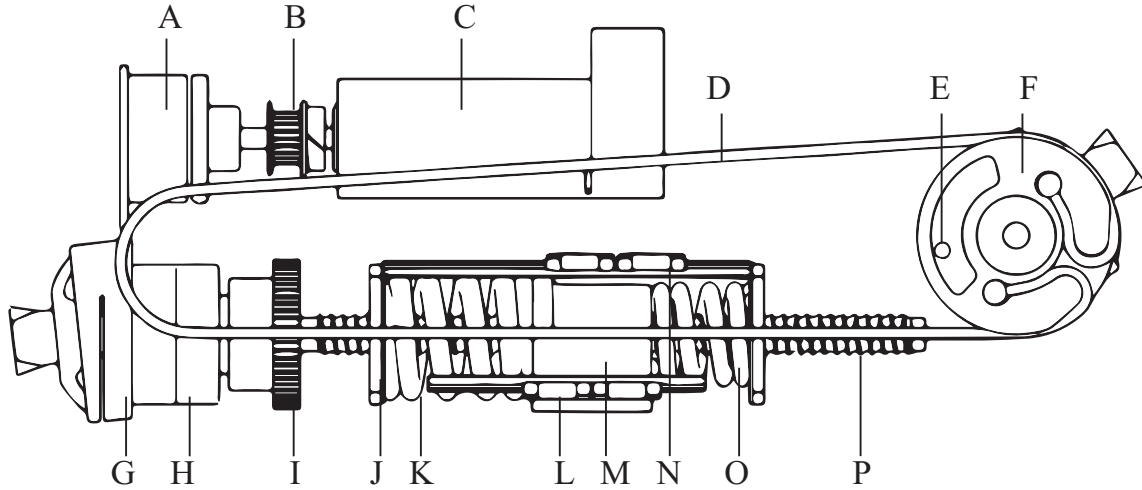
Fig. 5. The major components of the clutchable series-elastic actuator knee are depicted: (A) electromagnetic clutch; (B) motor timing pulley; (C) Maxon EC-40 4-Pole 200 W brushless motor; (D) steel drive cable; (E) internal hard stop; (F) knee pulley and joint; (G) distal pyramid with embedded load sensor; (H) paired 35° angular bearings; (I) ballscrew timing pulley; (J) series-elastic housing; (K) extension spring; (L) ball nut linear bearings; (M) ball nut; (N) series-elastic housing linear bearings; (O) flexion spring; (P) ballscrew.

internal hardstop. Placing the hardstop within the knee joint eliminated pinch points. The ballscrew bearings, series-elastic carriage linear bearings, knee joint and motor/clutch assembly were all mounted to a single, billet 6061-T6 aluminum body. SolidWorks Simulation was used to simulate the strength of the unibody under the weight of a 100 kg load (SolidWorks 2012, Dassault Systems, Waltham, Massachusetts). The simululation predicted a minimum safety factor of seven, meaning the structure would not yield before a load of seven times bodyweight. The layout of the CSEA within the aluminum unibody resulted in a compact (285 mm length) and lightweight (2700 g) device. The length of the CSEA Knee was within the first percentile male, and the mass was within the eighth percentile male (Winter, 1991; Byrd, 2005). The mass distribution of the CSEA Knee is shown in Table 3.

A custom load sensor was developed to detect the stance phase. The detection of the stance phase was important for stability and safety (see Section 4.2). Footswitches are typically used but are cumbersome to implement, since they require a wired connection between the the foot and the embedded module. Instead, the stance phase was detected by placing a force-sensing resistor (FSR) (model: A300-25, Tekscan, South Boston, MA) within a flexure in the distal pyramid. The sensor detected a combination of vertical loading and sagittal plane moment, and was only used to estimate gait cycle timing for control purposes. Figure 5 (callout G) shows the distal pyramid with a simple cantileavered flexure machined into the anteriorly facing side. A FSR was placed within the flexure and subsequently castable silicone (model: Mold Star 16 Fast, Smooth-On, Easton, Pennsylvania) was poured around the FSR. The castable silicone bonded the FSR to both sides of the flexure without creating a pre-load. When the flexure was

Table 3. Clutchable series-elastic actuator (CSEA) knee mass distribution.

| Part	Mass
SEA springs, housing, bearings	491 g
Structural housing	385 g
Brushless motor	300 g
Knee joint, pyramid, bearings	296 g
Ball screw, nut, bearings	287 g
Distal pyramid/Load sensor	195 g
Batteries	160 g
Clutch	100 g
Electronics	55 g
Motor and ball screw pulleys	41 g
Minor parts and wiring	390 g
Total	**2700 g**

compressed the load was transmitted through the silicone and FSR sensor. The FSR was connected in series with a 5 MΩ resistor in a voltage divider configuration. The voltage was read by the onboard data acquistion system, discussed in Section 4. An example of the load sensor voltage during a representative gait cycle is shown in Figure 6.

4. Electronics and control

4.1. Electrical hardware

The CSEA Knee prosthesis contained embedded systems responsible for fully autonomous operation. The system included modules for high-level state estimation, low-level brushless motor control, signal processing and sensing, communication and battery power (Figure 7). For design convenience, commercial components were chosen rather
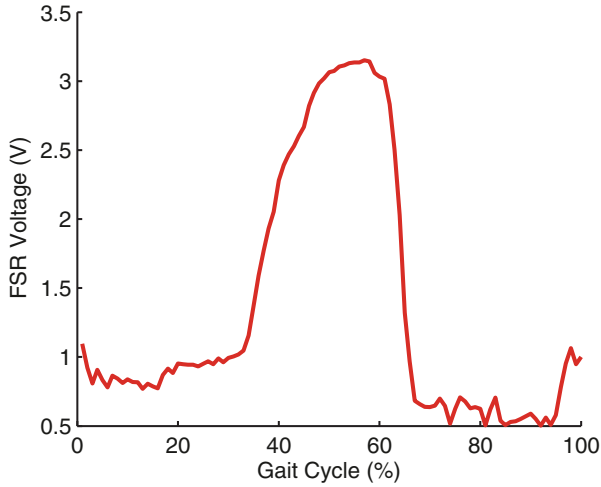
Fig. 6. The custom load sensor output during one gait cycle is depicted. The load sensor and voltage divider output approximately 0.5 V when unloaded. This value increased to 1 V at heel strike (0%). As a result of the orientation of the flexure, it was more sensitive to extension moments across the knee. A large extension moment was applied to the knee during the middle of stance (25%), which led to a load sensor output of 3 V. Subsequently, the load sensor fell to 0.5 V following the removal of the extension moment, where it remained until heel strike.

than the development of custom embedded systems. The high-level control was implemented on a commercial single-board computer (model: Raspberry Pi Version B, Raspberry Pi Foundation, Cambridgeshire, UK). The computer was equipped with an 800 MHz ARM11 processor, 512 MB SDRAM, with Linux Debian and required 3.5 W. It was chosen for its communication and input/output (I/O) options as well as its cost, form factor and active development community. This high-level controller was responsible for state estimation, data acquisition and storage as well as master command of the low-level brushless motor drive; all functionality of the high-level controller was implemented in Python. The high-level controller communicated wirelessly to a laptop PC via a wireless internet adapter (model: EW-7811un, Edimax Technology Co., New Taipei City, TW). The laptop PC was only used for initiation of the controller state machine and tuning control parameters (i.e. knee operation was autonomous). Data acquisition and logging occurred at 100 Hz, which stored data on a 32 GB secure digital card. The high-level controller communicated with a smart light-emitting diode (LED) indicator (model: minM, ThingM Corp., San Francisco, CA), inertial measurement unit (model: ADXL345 accelerometer, Analog Devices Inc., Norwood, MA; model: ITG-3200 gyroscope, InvenSense Inc., Sunnyvale, CA) and an analog-to-digital converter via an inter-integrated circuit (I^2C) bus at 500 kbaud. A four-channel 16-bit analog-to-digital converter (model: ADS1115, Texas Instruments, Dallas, TX) was used to interface with analog sensors. The analog sensors included an absolute encoder (model: MA3, US Digital, Vancouver, WA) that sensed knee angle with a resolution of 6×10^{-3} radians, as well as the force-sensitive resistor-based load sensor. The high-level controller updated at a frequency of 100 Hz. Low-level control
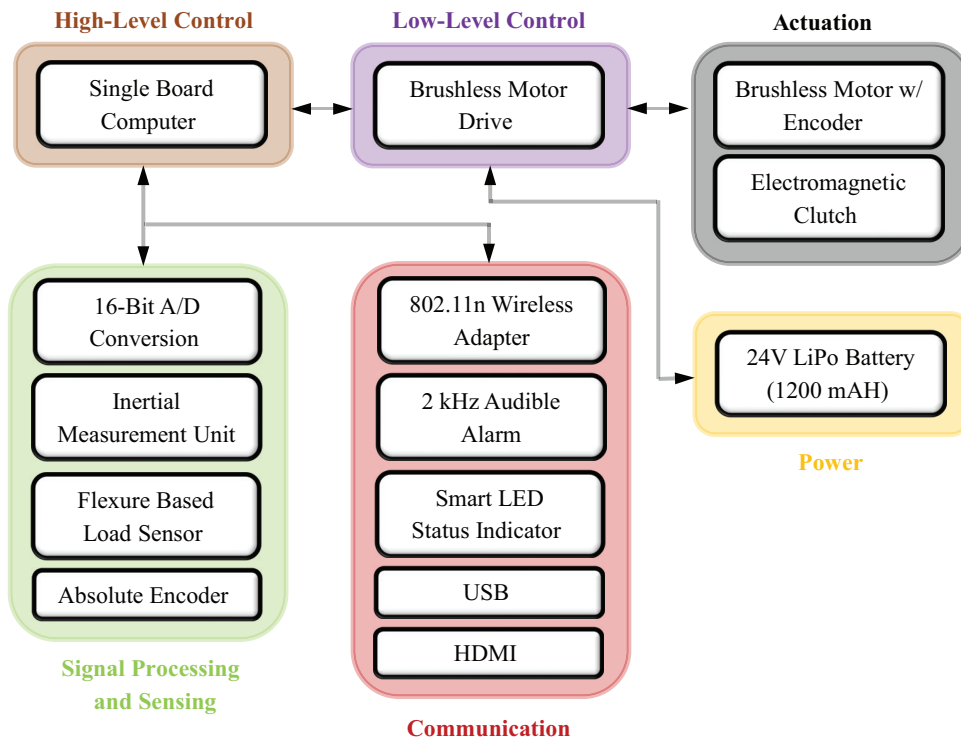
Fig. 7. Diagram showing embedded modules within the clutchable series-elastic actuator knee.
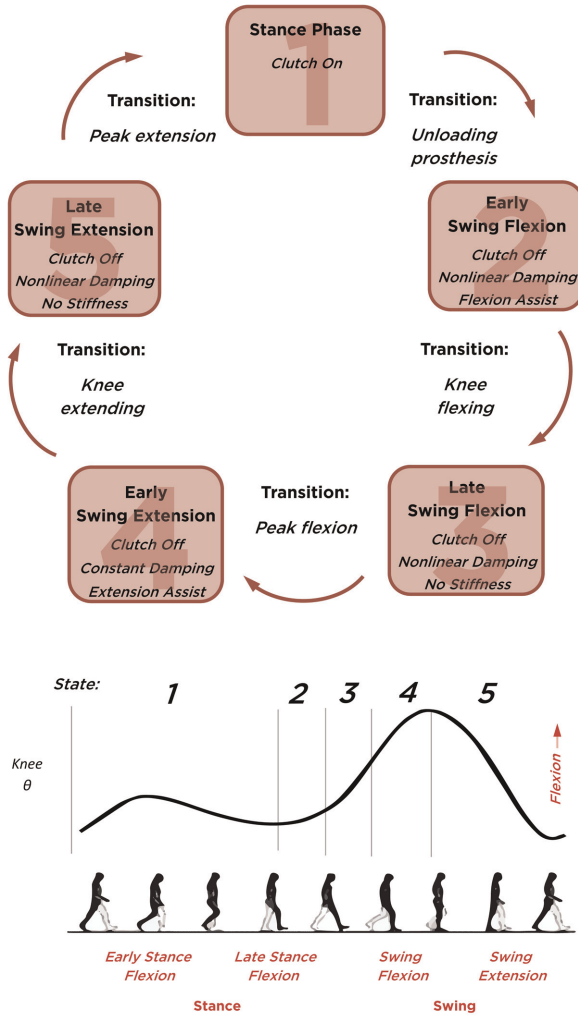
Fig. 8. Top: state machine depicted with general indication of state purpose and transitions. Bottom: able-bodied knee angle profile shown as a function of gait cycle. Each state location is denoted and stance phase is comprised solely by state one. In addition, sub-portions of stance and swing phase are shown with their location in the gait cycle

was implemented using a 400 W commercial brushless motor drive with four quadrant capabilities (model: IPOS 4808VX, Technosoft Motion, Neuchâtel, CH). The drive was chosen for its compact size, I/O options and current capabilities (8 A continuous, 20 A peak). To promote electrical efficiency, the drive is able to regenerate power during the second and fourth quadrants of the motor's torque-velocity profile. An impedance control architecture was implemented, permitting modulation of knee stiffness, damping and equilibrium position parameters. The drive's impedance control loop updated at 2 kHz with an inner current loop that updated at 10 kHz. The high-level controller communicated bidirectionally with the drive. The impedance parameters were updated by the high-level controller at 100 Hz and the drive sent values of motor current, voltage and position to the high-level controller. Communication between the controllers was via RS-232 at

115.2 kbaud. All power management was implemented on the drive, which supplied regulated 5 V to the high-level controller. Power was supplied by a six-cell 24V lithium polymer battery with a 1200 mAH capacity.

4.2. State estimation and control

Implemented on the high-level controller, a finite-state machine governed walking behavior of the CSEA Knee. Each state consisted of parameterized knee impedance including joint stiffness, damping and set-point values, as well as transition criteria. During operation, the states are concatenated to produce seamless locomotion behavior. An impedance-based controller was chosen to cooperatively render joint impedance with the integrated series compliance within the CSEA mechanism. In addition, such controllers have had much success in previously developed robotic prostheses, both within our group (Au and Herr, 2008; Martinez-Villalpando and Herr, 2009) and abroad (Sup et al., 2009). To estimate location within the gait cycle, the high-level controller used the onboard sensor information, and transitions were imposed as specified criteria were satisfied. The controller used knee angle and angular velocity, as well as the flexure-based load sensor voltage to discriminate between states. The angular velocity was calculated using the finite difference derivative method with a two-point weighted moving average filter (weights = [2, 1]).

The gait cycle was divided into five states: (1) stance phase; (2) early swing flexion; (3) late swing flexion; (4) early swing extension; and (5) late swing extension (Figure 8), with each state having separate impedance representations. State two includes the late-stance flexion portion of stance phase while both feet are in contact with the ground. The state-dependent impedance functions were inspired by investigation of the torque-angle and torque-angular velocity relationships of the able-bodied knee, as well as the joint's mechanical power profile (based on the work of Martinez-Villalpando (2012)). State one was comprised of stance phase, and began with heel contact of the prosthesis and continued until weight began to transition to the non-affected side (i.e. double support). During state one, the clutch was activated, rendering knee stiffness as the series compliance within the CSEA mechanism. The purpose of this phase was to provide the appropriate knee torque-angle relationship at the reduced electrical cost of the electromagnetic clutch. As unloading commenced, the controller transitioned to the swing flexion states (two and three). The purpose of these states was to supply positive power to initially flex the knee and remove energy as the knee approached peak swing flexion. Positive mechanical power was provided in state two by a unidirectional virtual spring (flexion torque only) that was instantaneously preloaded. The power added was consistent with the power profile of the able-bodied knee. During state three, energy was removed by a nonlinear damping impedance. The nonlinear impedance was implemented as a quadratically

Table 4. State impedance laws.

State	Clutch	Control law	Gait phase
1	On	$\tau = b\dot{\theta}$	Stance
2	Off	$\tau = k(\theta - \theta_k) + (b_1(\theta - \theta_b)^2 + b_2)\dot{\theta}$	Early swing flexion
3	Off	$\tau = (b_1(\theta - \theta_b)^2 + b_2)\dot{\theta}$	Late swing flexion
4	Off	$\tau = k(\theta - \theta_k) + b\dot{\theta}$	Early swing extension
5	Off	$\tau = (b_1(\theta - \theta_b)^2 + b_2)\dot{\theta}$	Late swing extension

Table 5. State transition criteria.

State	Transition criteria	Transition variables		Gait phase
1	$V_Z < 0.9 V_{max}$	N/A	N/A	Stance
2	$\theta > \theta_{52}$	θ_{52}	0.62 rad	Early swing flexion
3	$\dot{\theta} < \|\dot{\theta}_{53}\|$ or	$\dot{\theta}_{53}$	0.09 rad/s	Late swing flexion
	$\theta > \theta_{53}$	θ_{53}	0.62 rad	
4	$\theta > \theta_{54}$	θ_{54}	0.52 rad	Early swing extension
5	$\dot{\theta} < \|\dot{\theta}_{55}\|$ or	$\dot{\theta}_{55}$	0.09 rad/s	Late swing extension
	$\theta < \theta_{55}$	θ_{55}	0.07 rad	

increasing damping value as a function of knee angle. As the knee reached peak swing flexion, the controller transitioned to the swing extension states (four and five). During state four, an initial positive power phase extended the knee as a unidirectional virtual spring (extension torque only) that was preloaded with a 75 ms ramp in equilibrium position angle; the purpose of this ramp was to more gently apply the extension torque and increase comfort. Similarly, the positive power phase added by the virtual spring can be observed in the able-bodied knee power profile. As the knee extended, the controller transitioned to state five. The purpose of state five was to decelerate the leg as the knee extended prior to heel contact. Similar to state three, the deceleration was imposed using a quadratically increasing damping impedance. A secondary purpose of state five was to store energy in the flexion spring as the motor provided a substantial deceleration (flexion) torque. In other words, as the leg decelerated, the applied flexion torque compressed the flexion spring. The compression of this spring promoted efficient energy exchange from the flexion spring to the extension spring as the knee transitioned to early-stance phase knee flexion (state one). The control laws and transition criteria are provided in Tables 4 and 5, respectively. It should be noted that state one includes a damping term to prevent oscillations if the clutch is disengaged when there is nonzero compression of the series spring. Finally, the rendered knee impedance at the joint will include the stiffness ($k_s = 240$ Nm/rad) in series with the motor's impedance.

5. Experimental testing

To quantify the efficacy of the CSEA Knee, the robotic prosthesis was tested by a unilateral above-knee (transfemoral) amputee. The purpose of the clinical testing was to test the device's ability to promote early-stance flexion obtained through the compression of the series compliance, as well as the energy efficiency that results from using the clutch to provide the reaction torque. Early-stance knee flexion is important because it may reduce impact loading during early stance, and the metabolic energy required to walk (Inman and Eberhart, 1953; Gard and Childress, 2001). The testing was performed by characterizing the device's joint kinematic and kinetic profiles, as well as the electrical and mechanical energy that resulted.

Experiments were performed to test the performance of the CSEA Knee during level-ground locomotion. The study was approved by the MIT Committee On the Use of Humans as Experimental Subjects and informed consent of the participant was obtained. The participant was a 48-year-old male (height: 1.83 m, weight: 89.3 kg) that was 39 years post amputation, whose residual limb was 43% of the length of his sound side (measured from the greater trochanter to the lateral epicondyle). For daily use, the participant used a suction socket suspension with a microprocessor-controlled knee and a vertical shock energy return prosthetic foot. During testing, a powered ankle prosthesis (BiOM Inc., Bedford, MA) was used in combination with the CSEA Knee (Figure 9). Since the CSEA Knee design was inspired by the biomechanics of the intact human knee joint during locomotion, a powered ankle prosthesis was chosen that closely mimics the natural behavior of the human ankle joint. Initially, the subject was fitted with the prostheses by a certified prosthetist who subsequently tuned the BiOM using the commercially available application. During the BiOM tuning process, the control program of the ankle was adjusted to produce

Fig. 9. Anterior view of the clutchable series-elastic actuator (CSEA) knee shown with translucent protective cosmesis (a). Anterior and lateral views of the CSEA Knee with the BiOM powered ankle prosthesis (b). This configuration was used to test the CSEA Knee during walking.

Table 6. Impedance controller parameters.

Parameter	Values	Gait phase
b	25.0 Nms/rad	Stance
k	28.6 Nm/rad	Early swing flexion
θ_k	0.61 rad	
b_1	4.4 Nms/rad/rad^2	
θ_b	0.0 rad	
b_2	0.5 Nms/rad	
b_1	4.4 Nms/rad/rad^2	Late swing flexion
θ_b	0.0 rad	
b_2	0.5 Nms/rad	
k	24.3 Nm/rad	Early swing extension
θ_k	0.61 rad	
b	0.7 Nms/rad	
b_1	93.6 Nms/rad/rad^2	Late swing extension
θ_b	0.52 rad	
b_2	0.7 Nms/rad	

biological levels of net work. Lastly, a 0.1 rad flexion bias spacer was added by the prosthetist at the proximal knee attachment pyramid.

5.1. Parameter tuning

Prior to testing, the controller's impedance parameters were tuned to adjust the kinetic and kinematic profiles of the CSEA knee during locomotion. The participant walked on a treadmill at a self-selected speed (1.3 m/s, approximately 52 steps/minute) while the parameters were adjusted. The parameters were tuned using an iterative approach based on three criteria: (1) comparison of kinematic and kinetic

profiles to those observed from standardized biological datasets; (2) clinical input from the prosthetist; and (3) the level of comfort of the participant. The subject walked for approximately 1 minute while the gait parameters were quantified; during this time the prosthesis was fully autonomous and no tether was used. Following this assessment modifications were made to the parameters and the next iteration trial was subsequently completed. This process was repeated for approximately 6–8 iterations. Once the parameters were successfully tuned, the final impedance values were as shown in Table 6 with resulting stiffness and damping profiles for a representative stride as shown in Figure 10.

5.2. Walking testing

Following the determination of the controller parameter set, the participant walked with the CSEA Knee at the self-selected pace (1.3 m/s, 0.87 prosthesis steps/s). Three trials were collected where each trial consisted of the participant walking on the treadmill for three minutes. During each trial, the participant walked approximately 230 m (approximately 150 steps). Kinematic and kinetic data were acquired and stored using the integrated electronic modules. The mean torque-angle relationship (Figure 11) demonstrates the biological realism of the CSEA Knee. On average, the subject walked with 0.27 radians of early-stance phase knee flexion, which included the 0.1 radian flexion spacer. The mean flexion angle of the biological knee is 0.37 radians; thus, the CSEA Knee obtained approximately 73% of the flexion observed in biological
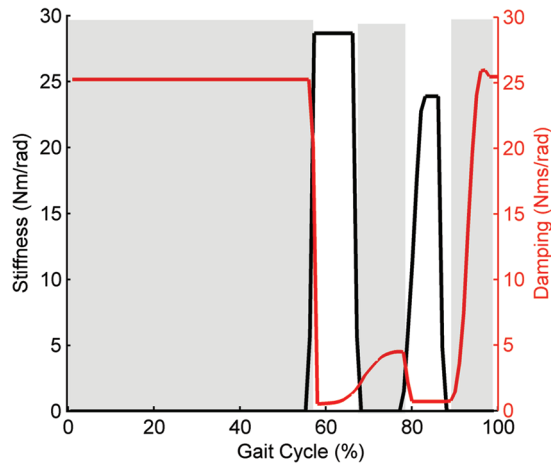
Fig. 10. Stiffness and damping profiles that result from the impedance-based state machine. Stiffness values are shown on the left axis and damping values are shown on the right axis; both are in terms of their effect on the knee joint.
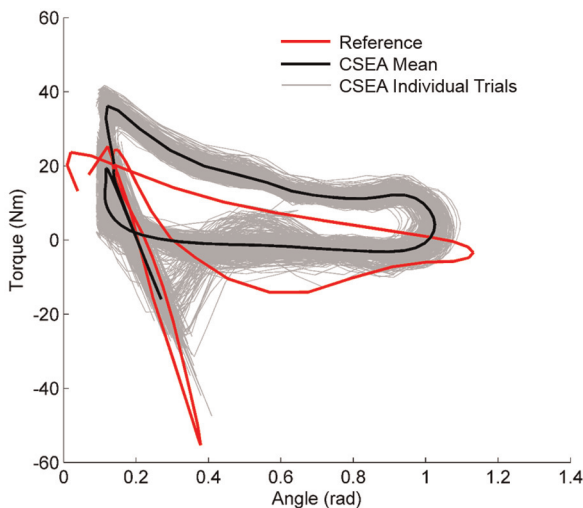
Fig. 11. The torque-angle profiles for the knee joint, shown for both the experimental participant (black, mean) as well as weight-matched standardized biological data (red, mean). The gray lines indicate the individual trials for the clutchable series-elastic actuator (CSEA) knee. Note the agreement of the mean profiles—the CSEA Knee obtained an average of 0.27 radians of early-stance flexion, approximately 73% of that seen in the biological knee.

data. In addition, the mean net work produced by the CSEA Knee was within 17% of weight-normalized biological data. The peak flexion angle of the CSEA Knee was 1.0 radian, compared to approximately 1.1 radians observed in human data.

The torque of the CSEA Knee was comparable to that observed in biological data as well. A peak torque of 15.5 Nm was observed during early-stance flexion (less than that of biological data because of the reduced peak stance flexion angle [Figure 11]). During the swing phase,
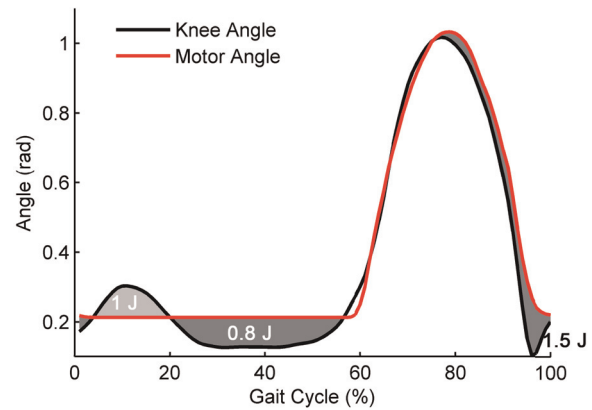

Fig. 12. Knee and motor angles shown for a representative stride (0% heel contact). Their difference denotes the deflection of the series compliance, which originally stores 1.5 J during late swing extension and transfers this energy during early-stance knee flexion. This figure highlights the exchange of energy between the two springs.

the CSEA Knee initially provided less torque when compared to biological data, but provided greater torque during swing extension. The deceleration torque provided by the CSEA Knee was used to regenerate substantial power during this portion of the gait cycle.

5.3. Mechanical energy transfer

Efficient mechanical energy storage both promotes early-stance knee flexion as well as reduces the electrical power needed during late-stance flexion. The knee angle and motor angle are shown in Figure 12, with the difference between the profiles denoting the compression of the flexion or extension springs. During late swing extension, the motor was decelerating the leg, providing substantial knee torque. This torque caused the mechanism's flexion spring to store mechanical energy, which was then transferred throughout stance phase. The energy stored in the flexion spring promoted stance phase knee flexion as the energy was transferred from the flexion spring to the extension spring (1 J, Figure 12). In other words, at stance initiation a flexion torque was provided by the compression of the flexion spring, which encouraged the participant to flex the knee. This is significant because transfemoral amputees often resist early-stance flexion as a result of previous passive prosthetic knees being unable to provide any early-stance flexion (i.e. if older prosthetic knees flexed during stance phase, they would buckle). Thus, the device's tendency to provide early-stance flexion is meaningful from a clinical perspective. Subsequently, as the knee exited early-stance knee flexion, the energy was transferred from the extension spring back to the flexion spring as the knee extended (0.8 J), prior to late-stance flexion. Lastly, as the knee began swing flexion, the energy stored in the flexion spring was released to aid in knee flexion. This transfer of energy highlights the role of the tuned series compliance
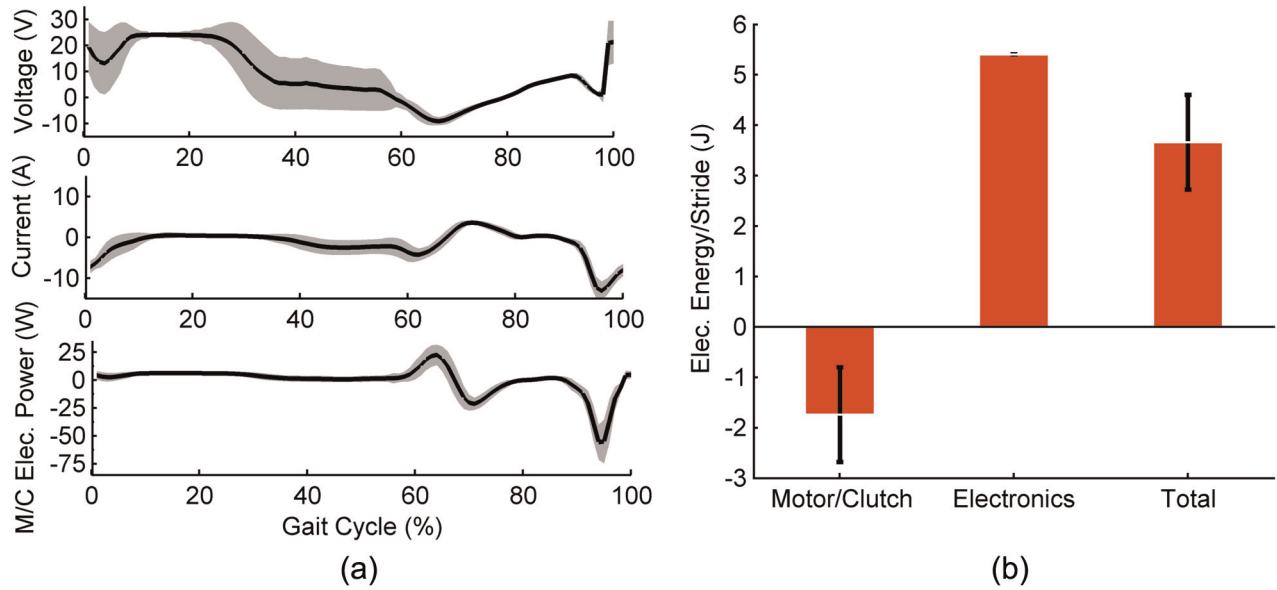
Fig. 13. (a) Profiles of the clutchable series-elastic actuator (CSEA) knee's total voltage, current and electrical power profiles during locomotion (combined motor and clutch). Note the substantial negative power region during late swing extension. The mean is shown in bold and the standard deviation is shown in translucent. (b) The mean electrical energy per stride shown for the electromechanical components (–1.8 J), the electronic modules (5.4 J) and the net total energy consumed (3.6 J). Standard deviations are shown as error bars.

within the CSEA Knee to provide not only electromechanical efficiency, but also potential clinical benefits.

5.4. Power consumption

One of the main goals of the CSEA Knee was to lower electrical energy consumption for elastically conservative regions of a movement task. This design objective was critical because robotic prostheses must be energetically autonomous, using onboard batteries that make the device substantially heavier and more cumbersome. In this work, negative electrical power refers to the absorption of energy from the environment (i.e. could be used to charge the power source), whereas positive electrical power refers to energy consumed to do work on the environment.

The net electrical energy consumed by the CSEA Knee was reduced during walking. The electromechanical components of the CSEA Knee (i.e. motor and clutch) generated 1.8 J of electrical energy during each stride. The electronic modules consumed 5.4 J/stride at 4.8 W. Thus, the net electrical energy consumption was 3.6 J/stride during locomotion (Figure 13). The energy generated by the electromechanical components was a result of utilizing the motor as a generator, and was facilitated by the energy-efficient nature of the transmission as well as the low-power clutch that reduced the electrical energy required by the motor (Figure 13(a)). This is consistent with previous work that showed 5 W of electrical energy generation from energy harvesting knee orthoses worn by able-bodied subjects during locomotion (Donelan et al., 2008). The electronic modules were considered separate from the electromechanical components, as the modules were commercial electronic components whose functionality could

easily be reduced to a custom, power-optimized embedded system that would consume substantially less electrical energy. For example, the quiescent electrical power consumption of the BiOM powered ankle prosthesis was measured to be 2–2.5 W, a 50% reduction from the electronic modules in the CSEA Knee.

The net electrical energy consumed by the CSEA Knee during locomotion is an order of magnitude less than previously published robotic knee prostheses. Sup et al. (2009) demonstrated a robotic knee-ankle prosthesis, of which the knee alone used approximately 21 W during locomotion (corresponding to 23 J/stride), including energy consumption by the electronics. The substantial energetic savings of the proposed knee prosthesis is a result of the CSEA mechanism—a low-power clutch was used to provide the reactionary torque during an elastically conservative task. To further reduce the power consumed by the clutch, the peak holding torque may be reduced to only that which is necessary during stance flexion. For example, by reducing the peak holding torque by 50%, the current can be reduced to approximately 125 mA and the electrical power consumed by the clutch would be reduced by a factor of four. In addition, the lightweight and efficient mechanical design of the CSEA contributes its energetic economy. Thus, the power source onboard the CSEA Knee can be smaller and lighter compared to previously developed devices.

Using the onboard battery within the CSEA Knee, an amputee user could walk throughout their community without recharging. The power source for the CSEA Knee was provided by a 1200 mAh LiPo battery (28.8 Wh) that weighed 160 g. Assuming consistent energy characteristics, an amputee with the CSEA Knee prosthesis could walk

approximately 30,000 strides (i.e. steps of the prosthesis) or 40 km at the participant's preferred speed, for a duration of 8.7 hours. In addition, considering only the quiescent power consumed by the electronic modules, an amputee could stand with the CSEA Knee prosthesis for approximately 6 hours (operating with only significant viscosity during standing) with a single charge of the battery. The total operating duration for walking is greater than the potential duration of standing alone as a result of the energy-generating nature of walking with the CSEA Knee prosthesis. Finally, the usage time required to drain the battery could easily be extended by creating a low-power (sleep) state of the prosthesis that could be implemented during relaxed modes (i.e. sitting).

6. Design limitations

The clutch and series elasticity within the CSEA mechanism introduce limitations. As with all SEAs, the series compliance within the CSEA Knee limits the maximum impedance that the device is able to render. As a result, the CSEA Knee is limited to biomechanical activity modes that are within the bandwidth of the CSEA mechanism (with k_s = 240 Nm/rad). In addition, when the clutch is activated the motor is not able to provide additional torque—a drawback not seen in parallel spring designs. Control intelligence could be added to the CSEA Knee that deactivates the clutch and uses the motor to apply the required torque if needed; for example, this may be necessary during obstacle avoidance or fall recovery.

The torque-angle behavior of the CSEA Knee is fixed during early-stance knee flexion, only able to render the 240 Nm/rad. As such, it may not vary stiffness with other parameters, including walking speed. Fortunately, biological knee quasi-stiffness has been shown to be relatively constant across walking speeds (Shamaei et al., 2013).

7. Conclusion

This paper provided the theory and design implementation of a CSEA in a robotic knee prosthesis. The purpose of the CSEA was to leverage a tuned series compliance with a low-power clutch to provide normal biomechanics with minimal electrical energy consumption. Since the CSEA Knee was powered, it provides the clinical capabilities to support a wide array of net-positive locomotion modes not available with traditional passive prosthetic knees. The mechanical design was detailed and resulted in a device that was lighter than the eighth percentile and shorter than the first percentile male shank segment. Experimental results with a unilateral transfemoral amputee showed biomechanically accurate knee torque-angle behavior, agreeing within 17% of the net work and 27% of the stance flexion angle produced by the biological knee. The CSEA Knee was electrically efficient; the electromechanical components of the mechanism (motor and clutch) generated energy during locomotion (1.8 J/stride), while the electronic modules consumed 5.4 J/stride. Hence, the net energy consumption was 3.6 J/stride. Future

work includes the development of a custom, low-power embedded system, a comprehensive gait study investigating the clinical benefits of the CSEA Knee as well as the expansion of the CSEA architecture to other biomechanically relevant joints for bionic prosthesis development.

Authors' note

The first two authors contributed equally to this work.

References

Albu-Schaffer A, Eiberger O, Grebenstein M, et al. (2008) Soft robotics. *IEEE Robotics & Automation Magazine* 15: 20–30.

Au S and Herr H (2008) On the design of a powered ankle-foot prosthesis. The Importance of series and parallel motor elasticity. *IEEE Robotics and Automation Magazine* 15: 52–59.

Au SK, Weber J and Herr H (2009) Powered ankle–foot prosthesis improves walking metabolic economy. *IEEE Transactions on Robotics* 25: 51–66.

Byrd A (2002) *The Measure of a Man and Woman: Human Factors in Design*. Hoboken: Wiley.

Christensen B, Ellegaard B and Bretler U (1995) The effect of prosthetic rehabilitation in lower limb amputees. *Prosthetics and Orthotics International* 19: 46–52.

Dilworth P, Herr HM and Paluska DJ (2006) Artificial human limbs and joints employing actuators, springs, and variable-damper elements. US Patent Application 11/395,448.

Donelan JM, Li Q, Naing V, et al. (2008) Biomechanical energy harvesting: generating electricity during walking with minimal user effort. *Science* 319: 807–810.

Endo K, Paluska D and Herr H (2006) A quasi-passive model of human leg function in level-ground walking. In: *IEEE/RSJ international conference on intelligent robots and systems*, pp. 4935–4939.

Gard SA and Childress DS (2001) What determines the vertical displacement of the body during normal walking? *JPO: Journal of Prosthetics and Orthotics* 13: 64–67.

Geerooms J, Flynn L, Jimenez-Fabian R, et al. (2013) Ankle-knee prosthesis with powered ankle and energy transfer for CYBER-LEGs α-prototype. In: *2013 IEEE international conference on rehabilitation robotics (ICORR), IEEE*, pp. 1–6.

Gitter A, Czerniecki J and Weaver K (1995) A reassessment of center-of-mass dynamics as a determinate of the metabolic inefficiency of above-knee amputee ambulation. *American Journal of Physical Medicine and Rehabilitation* 74: 337–338.

Ha KH, Varol HA and Goldfarb M (2011) Volitional control of a prosthetic knee using surface electromyography. *IEEE Transactions Biomedical Engineering on* 58: 144–151.

Haeufle D, Taylor M, Schmitt S, et al. (2012) A clutched parallel elastic actuator concept: towards energy efficient powered legs in prosthetics and robotics. In: *IEEE RAS & EMBS international conference on biomedical robotics and biomechatronics (BioRob)*, pp. 1614–1619.

Inman VT and Eberhart HD (1953) The major determinants in normal and pathological gait. *The Journal of Bone & Joint Surgery* 35: 543–558.

Jaegers SMHJ, Arendzen JH and de Jongh HJ (1995) Prosthetic gait of unilateral transfemoral amputees: a kinematic study. *Archives of Physical Medicine and Rehabilitation* 76: 736–743.

Johansson JL, Sherrill DM, Riley PO, et al. (2005) A clinical comparison of variable-damping and mechanically passive prosthetic knee devices. *American Journal of Physical Medicine and Rehabilitation* 84: 563–575.

Kapti AO and Yucenur MS (2006) Design and control of an active artificial knee joint. *Mechanism and Machine Theory* 41: 1477–1485.

Kaufman K, Levine J, Brey R, et al. (2007) Gait and balance of transfemoral amputees using passive mechanical and microprocessor-controlled prosthetic knees. *Gait and Posture* 26: 489–493.

Lagoda C, Schouten AC, Stienen AHA, et al. (2010) Design of an electric series elastic actuated joint for robotic gait rehabilitation training. *IEEE RAS and EMBS international conference on biomedical robotics and biomechatronics (BioRob)*, pp. 21–26.

Legro MW, Reiber G, Aguila M, et al. (1999) Issues of importance reported by persons with lower limb amputations and prostheses. *Journal of Rehabilitation Research and Development* 36.

Lemaire ED and Fisher FR (1994) Osteoarthritis and elderly amputee gait. *Archives of Physical Medicine and Rehabilitation* 75: 1094.

Martinez-Villalpando EC (2012) *Design and Evaluation of a Biomimetic Agonist-Antagonist Active Knee Prosthesis*. Cambridge, MA: School of Architecture and Planning, Massachusetts Institute of Technology.

Martinez-Villalpando EC and Herr H (2009) Agonist-antagonist active knee prosthesis: A preliminary study in level-ground walking. *Journal of Rehabilitation Research and Development* 46: 361–373.

Martinez-Villalpando EC, Mooney L, Elliott G, et al. (2011) Antagonistic active knee prosthesis. A metabolic cost of walking comparison with a variable-damping prosthetic knee. In: *annual international conference of the IEEE engineering in medicine and biology society (EMBC 2011)*, pp. 8519–8522.

Martinez-Villalpando EC, Weber J, Elliott G, et al. (2008) Design of an agonist-antagonist active knee prosthesis. In: *2nd IEEE RAS & EMBS international conference on biomedical robotics and biomechatronics (BioRob 2008)*, pp. 529–534.

Morgenroth DC, Gellhorn AC and Suri P. (2012) Osteoarthritis in the disabled population: a mechanical perspective. *PM&R* 4: S20–S27.

Morgenroth DC, Orendurff MS, Shakir A, et al. (2010) The relationship between lumbar spine kinematics during gait and low-back pain in transfemoral amputees. *American Journal of Physical Medicine and Rehabilitation* 89: 635–643.

Ossur. *The Power Knee*. Available at: http://bionics.ossur.com/Products/POWER-KNEE/SENSE (accessed May 2014).

Pratt G, Williamson M, Dillworth P, et al. (1997) Stiffness isn't everything. In: *experimental robotics IV*, pp. 253–262.

Pratt GA and Williamson MM (1995) Series elastic actuators. In: *proceedings of 1995 IEEE/RSJ international conference on intelligent robots and systems 95. 'Human robot interaction and cooperative robots'*, 1, pp. 399–406.

Pratt J, Krupp B and Morse C (2002) Series elastic actuators for high fidelity force control. *Industrial Robot: An International Journal* 29: 234–241.

Robinson DW, Pratt JE, Paluska DJ, et al. (1999) Series elastic actuator development for a biomimetic walking robot. In: *proceedings of the 1999 IEEE/ASME international conference on:advanced intelligent mechatronics*, pp. 561–568.

Rouse EJ, Gregg RD, Hargrove LJ, et al. (2013) The difference between stiffness and quasi-stiffness in the context of biomechanical modeling. *IEEE Transactions on Biomedical Engineering* 60: 562–568.

Segal AD, Orendurff MS, Klute GK, et al. (2006) Kinematic and kinetic comparisons of transfemoral amputee gait using C-Leg® and Mauch SNS® prosthetic knees. *Journal of Rehabilitation Research and Development* 43: 857.

Sensinger JW (2006) Improvements to series elastic actuators. In: *proceedings of the 2nd IEEE/ASME international conference on mechatronic and embedded systems and applications*, pp. 1–7.

Sensinger JW and Weir RF (2005) Design and analysis of a non-backdrivable series elastic actuator. In: *9th international conference on rehabilitation robotics (ICORR 2005)*, pp. 390–393.

Sensinger JW and Weir RF (2008) User-modulated impedance control of a prosthetic elbow in unconstrained, perturbed motion. *IEEE Transactions on Biomedical Engineering* 55: 1043–1055.

Shamaei K, Sawicki GS and Dollar AM (2013) Estimation of quasi-stiffness of the human knee in the stance phase of walking. *PLoS one* 8: e59993.

Smith DG (2007) Evaluation of function, performance, and preference as transfemoral amputees transition from mechanical to microprocessor control of the prosthetic knee. *Archives of Physical Medicine and Rehabilitation* 88: 207–217.

Sup F, Bohara A and Goldfarb M (2008a) Design and control of a powered transfemoral prosthesis. *The International Journal of Robotics Research* 27: 263–273.

Sup F, Varol HA, Mitchell J, et al. (2008b) Design and control of an active electrical knee and ankle prosthesis. In: *IEEE international conference on biomedical robotics and biomechatronics*.

Sup F, Varol HA, Mitchell J, et al. (2009) Preliminary evaluations of a self-contained anthropomorphic transfemoral prosthesis. *IEEE/ASME Transactions on Mechatronics* 14: 667–676.

Veneman J, Ekkelenkamp R, Kruidhof R, et al. (2006) A series elastic-and bowden-cable-based actuation system for use as torque actuator in exoskeleton-type robots. *The International Journal of Robotics Research* 25: 261–281.

Waters RL and Mulroy S (1999) The energy expenditure of normal and pathologic gait. *Gait and Posture* 9: 207–231.

Winter DA (1983) Biomechanical motor patterns in normal walking. *J of Motor Behavior* 15: 302–330.

Winter DA (1991) *The Biomechanics and Motor Control of Human Gait: Normal, Elderly and Pathological*. Waterloo: University of Waterloo Press.

Winter DA (2009) *Biomechanics and Motor Control of Human Movement*. Hoboken: Wiley.

Wolf EJ, Everding VQ, Linberg AA, et al. (2013) Comparison of the Power Knee and C-Leg during step-up and sit-to-stand tasks. *Gait and Posture* 38: 397–402.